DESIGN OF THE BEAM TRANSPORTATION LINE FROM THE LINAC TO THE 3-GEV RCS FOR J-PARC

T. Ohkawa#, JAERI, Ibaraki, Japan
M. Ikegami, KEK, Ibaraki, Japan

Abstract

The accelerators for the High-Intensity Proton Accelerator Facility Project, J-PARC, consist of a 180-MeV linac, a 3-GeV RCS (Rapid Cycling Synchrotorn), and a 50-GeV MR (Main Ring) [1]. L3BT is a beam transport line from the linac to the RCS.

To meet the requirement for the beam loss minimization, the L3BT does not only connect the linac to the 3GeV RCS, but also modifies the linac beam to be acceptable for the RCS. The required beam parameters at the injection point of the RCS are

Momentum spread < ±0.1% (100%) and

Transverse emittance < 4π mm*mrad (100%).

To achieve these beam qualities, the L3BT should have following functions: momentum compaction, transverse halo scraping and beam diagnostics.

In this paper, results of the design and beam simulation of the L3BT are presented.

DESIGN CONCEPT OF L3BT

The L3BT consists of the straight section, the arc section, the scraper section and the injection section. The magnetic fields of dipole and quadrupole magnets are restricted to be less than 0.5T to keep the Lorentz stripping losses within the acceptable level [2][3][4]. The design concept of each section is described in the following.

Straight section

The straight section consists of three parts: a matching section from the linac, a main beam transport line, and a matching section to the following arc section. The first debuncher cavity is located in the main part. In the second stage in which the linac energy is upgraded to 400 MeV, the most part of the main transport line will be replaced with ACS. To enable swift upgrade, the magnet configuration of the main part is designed to be the same with the final ACS lattice except that every other doublet is missing.

90 degree arc section

This section is composed of three DBA (Double Bend Achromatic) lattices. Since the focusing strength is sufficiently large and an amount of dispersion is small, the deteriorate effects due to both the space charge and a large dispersion on the transverse beam emittance are suppressed. The variation of the twiss parameters due to the space-charge effects is very small, indicating that any additional tuning of the focusing strength in the arc is not required during machine operation with varied peak beam currents.

Scraper sections

The scraper section is composed of simple four FODO cells. The phase advance of one FODO cell is set to about 45 degrees. Transverse scraper is installed after each Q-magnet to remove a transverse beam halo.

The second debuncher cavity is located before the first scraper to suppress the momentum spread.

Injection section

The injection section adjusts the transported beam to the required parameters for ring injection. The vertical bump magnet for the vertical painting injection is set at a position of π phase difference from the injection point.

BEAM SIMULATION

PARMILA code is used for the beam simulation. The input focusing data for the PARMILA are prepared by using TRACE3D. TRACE3D is the envelope analysis code including the space-charge effect and it has the parameter matching function.

Debuncher Effect

Two debunchers are set up in the L3BT. The debunchers are used to obtain the momentum spread of less than ± 0.1 % at the injection point of the RCS. Another effect of the debunchers is the energy centroid correction when the beam energy is shifted from the design value due to RF errors in the DTL and SDTL section. The simulation results are shown below.

The simulations from the MEBT to the RCS injection point are performed assuming RF errors in the DTL and SDTL. Assumed peak current is 30 mA and a 2D space-charge routine is adopted. The beam distribution based on the experiment and simulation result of RFQ is used as the initial beam distribution at the entrance of the MEBT [5]. Initial parameters are shown in Table 1.

Table 1: Initial parameters at the MEBT entrance

Number of particles	95322 particles
εx_0(rms)	0.212 π mm*mrad
εy_0(rms)	0.212 π mm*mrad
εz_0(rms)	0.091 π MeV*deg
εx_0(99.5%)	2.08 π mm*mrad
εy_0(99.5%)	2.05 π mm*mrad
εz_0(99.5%)	1.32 π MeV*deg

The design value for the first debuncher voltage is V_1= 1.1 MV, and that for the second debuncher voltage is V_2 =

#tohkawa@linac.tokai.jaeri.go.jp

0.45 MV. In the present arrangement of L3BT, the distance between the end of the SDTL and the center of the first debuncher is 53.126 m, the distance between the center of the first debuncher and that of the second debuncher is 167.831 m and the distance between the center of the second debuncher and the injection point of the RCS is 100.204 m.

The RF field amplitude and phase errors for each tank of the DTL and the SDTL are randomly generated within the range of ±1 % and ±1 deg. In addition, it is assumed that there are 6 deg phase and 6 % amplitude tuning errors for the debunchers.

At first, the simulations from the MEBT to the SDTL are performed for 100 random error cases. The obtained results are shown in Fig. 1.

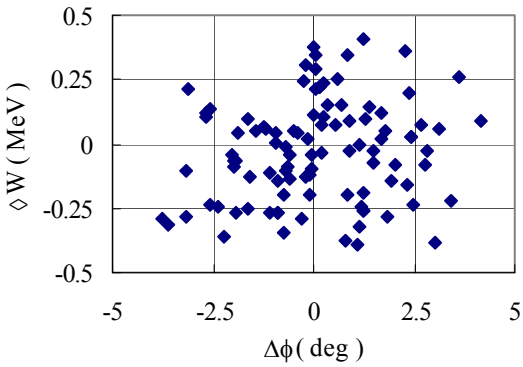

Figure 1: Simulated resutls of the phase and energy at the end of the SDTL.

Figure 1 shows that the beam energy and phase at the end of the SDTL are fluctuated within the range of ± 0.4 MeV and ± 4 deg. We shall concentrate on the cases that the energy at the end of the SDTL is maximum (ΔW=0.410 MeV (case 1)) and minimum (ΔW= -0.394 MeV (case 2)). Four patterns of errors shown in Table 2 are assumed as the tuning errors for the debunchers. In combining RF errors for the DTL and SDTL (case 1 and 2) and those for the debunchers (case a to d), we have performed eight end-to-end simulation runs to evaluate the overall effect of RF errors. In these cases, the space charge effect is calculated with three dimensions.

Table 2. Tuning errors for the Debunchers

	Unit	Case a	Case b	Case c	Case d
V_1	%	-6.0	-6.0	-6.0	-6.0
ϕ_1	deg	-6.0	6.0	-6.0	6.0
V_2	%	6.0	6.0	6.0	6.0
ϕ_2	deg	6.0	-6.0	-6.0	6.0

The calculation results of the phase and energy are shown in Table 3 and 4. In Table 3 and 4, W_{ref}, W_i, and W0 denote the design energy, output energy of SDTL, and the energy at the injection point, respectively. Δp/p is the momentum spread at the injection point. In the worst case, the momentum spread at the injection point of the RCS is about 0.12 % that is slightly larger than the requirement. The momentum spread at the injection point of the RCS is calculated by using 99.5% emittance.

We conclude from Table 3 and 4 that the momentum spread at the injection point of the RCS can be fluctuated within the range of ± 0.11 % with realistic RF errors.

Table 3. Simulation results of the phase and energy (The energy at the end of the SDTL is maximum (case1).)

	Unit	case 1-a	case 1-b	case 1-c	case 1-d
W_{ref}	MeV	181.034	181.034	181.034	181.034
W_i	MeV	181.445	181.445	181.445	181.445
V_1	MV	1.034	1.034	1.034	1.034
ϕ_1	deg	-127.7	-115.7	-127.7	-115.7
V_2	MV	0.477	0.477	0.477	0.477
ϕ_2	deg	-64.4	-123.4	-76.4	-111.4
W_o	MeV	181.012	180.796	180.938	180.872
Δp/p	%	-0.102	-0.112	-0.115	-0.096
		- 0.089	- -0.031	- 0.058	- -0.002

Table 4. Simulation results of the phase and energy (The energy at the end of the SDTL is minimum (case 2).)

	Unit	case 2-a	case 2-b	case 2-c	case 2-d
W_{ref}	MeV	181.034	181.034	181.034	181.034
W_i	MeV	180.640	180.640	180.640	180.640
V_1	MV	1.034	1.034	1.034	1.034
ϕ_1	deg	-63.3	-51.3	-63.3	-51.3
V_2	MV	0.477	0.477	0.477	0.477
ϕ_2	deg	-63.7	-121.9	-75.7	-109.9
W_o	MeV	181.260	181.045	181.179	181.115
Δp/p	%	0.027	-0.099	-0.010	-0.071
		- 0.109	- 0.106	- 0.097	- 0.120

Quadrupole Gradient Errors

Next, we consider the change of the beam parameters in the scraper section when systematic magnetic field errors are caused for all quadrupole magnets in L3BT due to fluctuations of their power supplies.

The simulations from the MEBT to the injection point of the RCS are performed with magnetic field errors systematically generated in L3BT. We evaluate the difference of beam loss caused by the change of the beam size at each scraper. It is assumed that the each scraper are set to the position of 0.65m downstream from the center of the each quadrupole magnets. A peak beam current is 30 mA and space charge effect is calculated with three dimensions. The same beam distribution shown in Table 1 is used as initial beam distribution at the entrance of the MEBT. We suppose that the charge conversion foils of each scraper are set up to scrape off particles outside the emittance of 4π mm*mrad.

At first, the simulations from the MEBT to the injection point of the RCS are performed with no magnetic field errors. The calculation results of normalized 99.5% emittance at the injection point of the RCS with or without scraper are shown in Table 5. The

beam distributions at the injection point of the RCS are shown in Figure 2. Table 5 shows that all the particles blown up over 4π mm*mrad are eliminated in scraper section and normalized 99.5% emittance at the injection point of the RCS meets the specification of less than 4π mm*mrad.

Table 5: Simulation results for normalized 99.5% emittance

	Unit	without scraper	with scraper
ΔG/G	%	0.0	0.0
εx	πmm*mrad	4.166	2.668
εy	πmm*mrad	3.668	2.599
εz	πMeV*deg	4.062	3.642
Δp/p	%	± 0.03	± 0.03

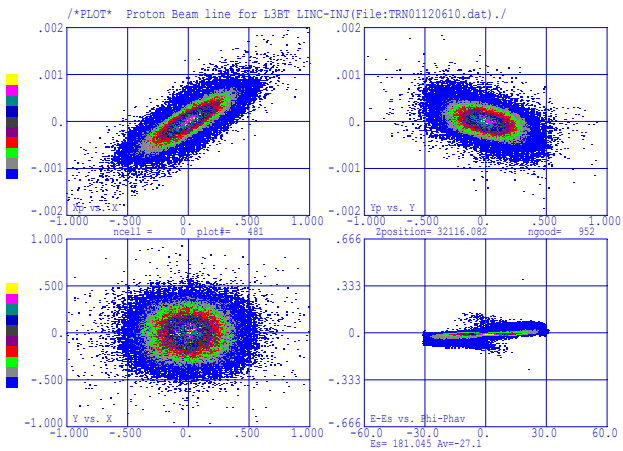

Figure 2(1/2) Beam distribution (RCS injection point, without scraper).

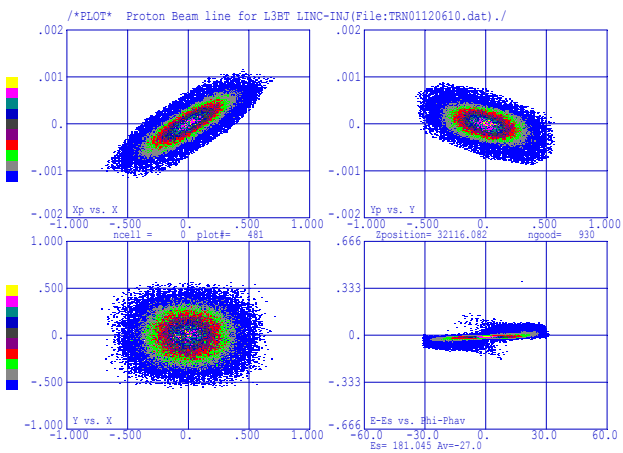

Figure 2(2/2) Beam distribution (RCS injection point, with scraper).

As for the quadruple magnetic field error, four cases (no error, 0.1%, 0.5%, and 1.0%) are considered. In each case, the same amount of gradient error is applied to all the quadrupoles. The number of collimated particles at each scraper is evaluated. The obtained results are shown in Table 6.

Table 6: Fraction of collimated beam

	Unit	case0	case1	case2	case3
ΔG/G	%	0.0	0.1	0.5	1.0
N_{LOSS}		2057	2054	2185	2165
Loss	%	2.159	2.157	2.295	2.276

When the magnetic field errors of 0.1% are systematically caused in each of quadrupole magnets of L3BT, the β function at each scraper changes within the range of ± 1.5% and the beam size changes within the range of ± 0.8%. It can be confirmed that the fraction of collimation at the scrapers is insensitive to the systematic gradient errors. When the magnetic field error becomes 0.5% or more, the amount of the fraction of collimation at the scrapers increases about 5-6%. Table 7 shows the simulation result of normalized 99.5% emittance at RCS injection point.

Table 7: Simulated results of normalized 99.5% emittance

	Unit	case1	case2	case3
ΔG/G	%	0.1	0.5	1.0
εx	πmm*mrad	2.704	2.750	2.726
εy	πmm*mrad	2.597	2.582	2.534
εz	πMeV*deg	3.693	3.651	3.762
Δp/p	%	± 0.03	± 0.03	± 0.03

Table 7 shows that the momentum spread at RCS injection point meets the specification though emittance in the z direction is slightly fluctuating with increasing systematic gradient errors.

SUMMARY

The simulations from the MEBT to the injection point of the RCS are performed with PARMILA with the RF errors in the DTL, SDTL and debunchers. Systematic quadrupole gradient errors are also considered, which can be caused due to fluctuations of the power supplies. It can be confirmed that the required beam parameters at the injection point of the RCS are nearly satisfied in all cases.

REFERENCES

[1] Y. Yamazaki(eds), "Accelerator Technical Design Report for J-PARC", KEK-Report 2002-13; JAERI-Tech 2003-044, March 2003.

[2] Andrew J. Jason, Daniel W Hudgings, Olin B van Dyck, IEEE TRANS. on Nucl. Sci., NS-28, 2704 (1981).

[3] M. S. Gulley et al., Phys. Rev. A, 53(5), 3201(1996)

[4] JHF Project Office, "JHF Accelerator Design Study Report", KEK Report 97-16 (JHF-97-10), 1998.

[5] Y. Kondo et al., Proc. 28th Linear Accelerator Meeting in Japan, Tokai, July 2003, TB-2.